# Polymer functionalization through an enzymatic process: intermediate products characterization and their grafting onto gum Arabic

Marie E. Vuillemin*, Lionel Muniglia*, Michel Linder*, Sabine Bouguet-Bonnet♦, Sophie Poinsignon♦, Raphael Dos Santos Morais*, Blandine Simard*, Cédric Paris†*, Florentin Michaux*, Jordane Jasniewski*

Corresponding author: jordane.jasniewski@univ-lorraine.fr

* Université de Lorraine, LIBio, F-54000 Nancy, France

† Université de Lorraine, PASM, SF4242, EFABA, F-54000 Nancy, France

♦ Université de Lorraine, CNRS, CRM2, F-54000 Nancy, France

KEYWORDS: gum Arabic, functionalization, phenol grafting, ferulic acid, oxidation product

ABSTRACT:

The modification of gum Arabic with ferulic acid oxidation products was performed in aqueous medium, at 30 °C and pH 7.5, in the presence of *Myceliophthora thermophila* laccase as biocatalyst. First, this study aimed to investigate the structures of the oxidation products of ferulic acid that could possibly be covalently grafted onto gum Arabic. HPLC analyses revealed that this reaction produced several oxidation products, whose structures were investigated using LC-MS/MS analyses (liquid chromatography-mass spectrometry with mass

fragmentation analyses) and NMR experiments. The chemical structure of one intermediate reaction product was fully elucidated as the 2-(4-hydroxy-3-methoxyphenyl)-4-[(4-hydroxy-3-methoxyphenyl) methylidene] cyclobutane-1, 3-dione, called by the authors cyclobutadiferulone.

Secondly, this study aimed to locate the grafting of the oxidation products onto gum Arabic by performing several NMR experiments. This study did not determine how much and specifically which oxidation products were grafted but some of them were undeniably present onto modified gum Arabic, close to the glucuronic acid C5 carbon or close to the galactose C6 carbon.

## 1. Introduction

Gum Arabic (GA) is a sticky exudate of air-solidified sap from the trunks or tree branches of Acacia trees such as *Acacia senegal* and *Acacia seyal*, which essentially provides a friable gum (Idris, Williams, & Phillips, 1998; McNamee, O'Riorda, & O'Sullivan, 1998; Nussinovitch, 1997). GA is mainly composed of D-galactose (39 to 42%), L-arabinose (24 to 27%), L-rhamnose (12 to 16%), D-glucuronic acid, 4-O-Methyl-β-D-glucuronic acid (15 and 16%) and a small amount of proteins (1.5 to 2.4%) (Idris *et al.*, 1998). The polysaccharides and proteins present in GA can be divided into three main fractions (Idris *et al.*, 1998; Williams *et al.*, 1990): arabinogalactan-peptide (AG), arabinogalactan protein (AGP) and glycoprotein (GP). These fractions differ in their molecular weight, protein content and chemical composition (Mahendran, Williams, Phillips, Al-Assaf, & Baldwin, 2008; Randall,

40 Phillips, & Williams, 1988; Randall, Phillips, & Williams, 1989; Sanchez *et al.*, 2008;
41 Sanchez *et al.*, 2017; Shi *et al.*, 2017).

42 Recently, several studies are the witness of a growing interest for the modification of
43 GA, especially aiming to improve its emulsifying properties (Pirestani *et al.*, 2017; Shi *et al.*,
44 2017; Wang, Williams, & Senan, 2014). However, those studies are only focusing on the
45 modification of the polysaccharide by chemical pathways. Some authors have investigated the
46 enzymatic pathway on other polysaccharides. Previous studies demonstrated that it was
47 possible to modify chitosan and pectin by grafting oxidation products of ferulic acid (OXP)
48 activated by a laccase from *Myceliophthora thermophila* (Aljawish *et al.*, 2012; Karaki *et al.*,
49 2017). Oxidation products were grafted to the amine groups (carbon C2 of glucosamine) of
50 chitosan (by formation of a Schiff base) and onto the carboxylic acids (carbon C6 of
51 galacturonic units) of pectin (by the formation of an ester bond), thus modifying many of their
52 properties (Aljawish *et al.*, 2016; Karaki, Aljawish, Muniglia, Humeau, & Jasniewski, 2016).
53 Native gum Arabic (NGA) contains both amine groups (from its arabinogalactan-protein
54 fraction) and carboxyl groups (bore by the polysaccharides from the arabinogalactan-peptide
55 fraction), so the OXP could be grafted onto either or both sites. Since the arabinogalactan-
56 peptide fraction is predominant in gum Arabic (88% against 10% for the arabinogalactan-protein
57 fraction) (Lopez-Torrez et al., 2015) and that the carboxyl groups are mainly responsible for gum
58 Arabic negative charge in solution, the grafting of oxidation products could be preferably
59 orientated towards the carboxyl groups. However, in previous studies on other polysaccharides, it
60 was shown that the grafting of phenolic compounds, even in very small quantities, had a
61 significant impact on the physico-chemical properties of these polymers (Aljawish et al., 2012;
62 Karaki et al., 2017). Therefore, even a grafting onto the small fraction of amine groups of gum
63 Arabic could explain the physico-chemical changes observed in a previous study on the

enzymatic modification of gum Arabic with ferulic acid oxidation products in the presence of *Myceliophthora thermophila* laccase as biocatalyst (Vuillemin *et al.*, 2020). This study showed that this functionalization changed GA properties and led to an increase of its antioxidant properties and led to the apparition of a glass transition closed to 39 °C. However, the study did not prove undeniably if the oxidation products of ferulic acid were grafted on GA or only adsorbed onto it.

The main issue with this approach is that the laccase-catalyzed oxidation of ferulic acid is currently not well-controlled. It generates highly reactive unstable radicals that can spontaneously reorganize and may lead to the formation of phenolic oligomers. Many structural changes, including oxidative decarboxylation, may occur, thus increasing the number of possible oxidation product structures. Only a few structures have been fully elucidated, most of the others have not been completely identified yet (Ralph, Quideau, Grabber, & Hatfield, 1994). Furthermore, the existing identification of such products rely mostly on hypothesis based on the products molecular weight obtained by liquid chromatography-mass spectrometry (LC-MS) measurements (Aljawish *et al.*, 2014; Carunchio, Crescenzi, Girelli, Messina, & Tarola, 2001; Karaki *et al.*, 2017). Yet, for one molecular weight, multiple structures could be proposed. Some studies have demonstrated that several structures of the same molecular weight could coexist, based on nuclear magnetic resonance (Ralph, Quideau, Grabber, & Hatfield, 1994). Thus, this study aimed on one hand to determine the chemical structure of the oxidation products obtained from the oxidation of ferulic acid initiated by the laccase of *Myceliophthora thermophila.* The functionalization of polysaccharides through enzymatic process is a complex matter because it would require an interaction between the enzyme and polysaccharide, which are generally difficult and limited due to the steric clutter associated with the size of the polymer. As a solution, the laccase-

mediated functionalization is proposed. In this enzymatic pathway, only the phenolic compound (i.e. ferulic acid) is initially supported by the enzyme to form reactive species (semi-quinones). These radicals are active species which can either condense with each other or react with nucleophilic function, such as amino groups or carboxyl groups present on the polysaccharide. This mechanism has already been widely studied and although the mechanism of the non-enzymatic reaction step is still poorly understood, experimental evidence supports the hypothesis that quinones can undergo different types of reaction with amines to yield either Schiff-bases or Michael-type adducts, as well as oligomer-forming reactions with other quinones (Kumar et al., 2000, Mustafa et al., 2005, Aljawish et al., 2012).

The study of the grafted products is complex, which is why the study was focused on the free products that are easier to study. The assumption was made that they would not be different with or without gum Arabic since the intermediate species are formed before reacting with the polysaccharide. However, it could not be excluded that some rearrangements happen afterwards and that they could differ depending on whether the oxidation products condense with each other or react with gum Arabic.

Those products were expected to be grafted either on the carboxyl or on the amine group of GA. This study aimed to prove the grafting of the oxidation products onto the polymer and to locate these chemical species on GA. HPLC, LC-MS/MS and NMR analysis were used to resolve the structure of reactions products coming from the ferulic acid oxidation by the laccase. Then, NMR spectroscopies have been performed to confirm the grafting of the oxidation products on the polysaccharide.

## 2. Experimental

## 2.1. Materials

Gum Arabic (GA) Instantgum AA from *Acacia senegal* was a gift from Nexira (France). Ferulic acid (purity about 99%) (FA), anhydrous sodium phosphate dibasic ($Na_2HPO_4$), anhydrous potassium phosphate monobasic ($KH_2PO_4$), trifluoroacetic acid (TFA), deuterated water and deuterated methanol were purchased from Sigma-Aldrich (France). Analytical grade methanol, ethanol, formic acid and acetonitrile were purchased from Carlo Erba (Milwaukee, WI, USA).

The enzyme used for the oxidation was commercialized as "Novozym® 51003" from Novozymes (Bagsvaerdt, Denmark). It is a fungal laccase from *Myceliophthora thermophila*, a polyphenol oxidase produced by submerged fermentation of a genetically modified *Aspergillus oryzae* (Berka *et al.*, 1997). The laccase activity was determined by following the apparition of the oxidation product of syringaldazine (the reference substrate for laccase activity determination). The laccase stock activity was 32 038 ± 1 322 $LAMU.g^{-1}$ (Laccase Myceliophthora $Units.g^{-1}$).

## 2.2. Methods

### 2.2.1. Functionalization of gum Arabic

The method used to functionalize GA through a ferulic acid oxidation was adapted from previous protocols (Aljawish *et al.*, 2012; Karaki *et al.*, 2017; Vuillemin *et al.*, 2020). 1 g of GA was dispersed in 45 mL of phosphate buffer (50 mM, pH 7.4). The dispersion was stirred at 450 rpm for 1 h at 30 °C. 5 mL of ferulic acid (50 mM) dissolved in methanol was added to the batch. Once the temperature was stable, 13.5 $LAMU.mL^{-1}$ of Novozym® 51003 was

133 added to trigger the reaction. The batch was then stirred at 30 °C for 50 min. 150 mL of
134 ethanol (96%) stored at -20 °C was then added to stop the reaction and separate the non-
135 functionalized GA from the functionalized GA. The obtained mixture containing
136 functionalized gum Arabic (FGA), non-grafted FA oxidation products (OXP) (soluble in the
137 phosphate buffer/ethanol mixture) and non-functionalized GA (insoluble in the phosphate
138 buffer/ethanol mixture) was then centrifuged at 12000 *g* for 20 min at 20 °C with a Beckmann
139 centrifuge (Beckman Coulter Inc., Villepinte, France). The precipitate contained non-
140 functionalized GA and a part of phosphate buffer salts (verified by FTIR measurements, data
141 not shown), whereas the supernatant contained the functionalized GA and the ferulic acid
142 oxidation products not grafted on GA.

143 The ethanol was then eliminated with a rotary evaporator BuchiR144 (Buchi SARL,
144 Rungis, France) at a boiling point of 40 °C at 175 mbar. Some amount of water from the
145 buffer solution was also evaporated by decreasing the pressure down to 72 mbar.

146 2.2.2. Preparation of ferulic acid oxidation products

147 For the preparation of ferulic acid oxidation products the same protocol as for the
148 functionalization of gum Arabic has been performed but without adding gum. Ferulic acid and
149 OXP were soluble in the mixture of methanol and phosphate buffer. However, at the end of
150 the reaction, 150 mL of ethanol (96%) stored at -20 °C was still added to stop the reaction and
151 to precipitate buffer salts. The supernatant contained the OXP.

152 2.2.3. Purification of the component

153 For FGA, the residual solution was dialyzed against ultrapure water with a high-grade
154 regenerated membrane (MWCO 10 000 Da from Membrane Filtration Products Inc.) to

155 eliminate excess salts from the buffer and non-grafted FA oxidation products (the oxidation
156 products are soluble in water up to 5% (Vuillemin *et al.*, 2020) and they have a molar mass
157 lower than 610 Da (Figure 2)). Dialysis was stopped when the conductivity outside the
158 membrane was equal to the one of ultrapure water, i.e. equal to 1.0 ± 0.2 µS.cm$^{-1}$. The same
159 method was used to eliminate excess salt from NGA. For the OXP, they were purified using
160 Sephadex PD-10 pre-packed desalting columns (with Sephadex G-25 resin, GE Healthcare,
161 Buckinghamshire, United Kingdom). 25 ml of ultrapure water was used to equilibrate the
162 column, after what 2.5 mL of solution of OXP in ultrapure water was added. After the sample
163 had entered the packed bed completely, 2.5 mL of ultrapure water was added again to the
164 column. The eluate that was collected contained the OXP, while the salts remained in the
165 column. The dialyzed FGA and NGA and the purified OXP were then freeze-dried. The
166 powders obtained were stored in a desiccator, in the dark, at 4 °C until use.

167 2.2.4. Solubilization of the products

168 The solutions were prepared by dissolving FGA, NGA or OXP in ultra-pure water. The
169 solutions were stirred at 400 rpm overnight at 4 °C to ensure total solubilization of the
170 products.

171

172 2.2.5. Color modification during the oxidation reaction

173 During the functionalization of GA and the oxidation of ferulic acid by the laccase from
174 *Myceliophthora thermophila*, a change of the color of the mixtures was observed. The color
175 evolution of the reaction medium was measured with a spectrocolorimeter CR-5-Konica
176 Minolta (Konica Minolta Sensing, Europe B.V.). Prior to each run, the device was calibrated

using two standards (white and black). Every 10 min, CIE (International Commission on Illumination) color parameters (L*, a* and b*) were measured by placing 4 mL of the reaction mixture in the spectrocolorimeter tank. L* defines lightness and ranges from 0% (black) to 100% (white). The a* parameter denotes the red/green value and b* the blue/yellow value. The color difference (ΔE) between two samples was obtained using Eq.1.

$$\Delta E = \sqrt{\Delta L^2 + \Delta a^2 + \Delta b^2} \qquad \text{(Eq. 1)}$$

2.2.6. Monitoring of the ferulic acid consumption during the oxidation reaction (HPLC)

The oxidation of ferulic acid during the enzymatic reaction was monitored by high performance liquid chromatography (HPLC) (Shimadzu LC10). 100 µL of the reaction medium was collected and placed in 2 mL microtubes containing 900 µL of pure methanol to stop the reaction. Prior to analysis, samples were filtered through a 0.2 µm syringe filter and half diluted in ultra-pure water. 5 µL was injected into the HPLC system. The separation was performed on a reversed-phase GRACE Apollo C18 chromatography column (150 x 2.1 mm - 5 µm). The elution method consisted of a two-phase gradient at a flow rate of 0.2 $mL.min^{-1}$: a phase A (ultra-pure water/methanol/TFA 80:20:0.1) and a phase B (100% methanol). The gradient used consisted in 2 min of 20% of phase B, then the proportion of phase B was raised from 20% up to 90% during 14 min. The proportion of B was maintained at 90% for 5 min and finally at 20% for 10 min. The UV-VIS absorbance was measured between 190 and 900 nm on a multichannel photo-diode-array detector (SPD-M10A VP). The results were recorded and processed by a chromatogram processing software (LC solution). The amount of AF was measured at its maximum absorption (322 nm) after making a standard ferulic acid calibration from 0.1 to 0.5 mM.

### 2.2.7. Measurement of the approximate Zeta potential

The approximate Zeta potential of FGA and NGA (1.00% w/v) were calculated from measurement of the electrophoretic mobility at 25 °C, at pH 5.5, using a Zetasizer Nano-ZS instrument and DTS1070 disposable zetacell (Malvern Panalytical, United Kingdom) equipped with a He/Ne ion laser ($\lambda$= 532 nm). Measurements were collected on a detector at 173°. The instrument determined the Zeta potential with the Smoluchowski equation (Jayme, Dunstan, & Gee, 1999). All measurements were made in triplicate.

### 2.2.8. Structural characterization of the modified gum Arabic: Nuclear magnetic resonance analyses

Native gum Arabic (NGA) and functionalized gum Arabic (FGA) were characterized by NMR. They were solubilized in deuterated water at concentrations of 5.0% and 4.5% w/v, respectively. The solutions were then analyzed by NMR to determine their molecular structure and the proximity of the atoms from each other, by using a combination of 1D and 2D NMR techniques. Experiments were performed on a spectrometer operating at 9.4 Tesla (Bruker Avance III, frequencies of 400 Mhz and 100.6 MHz for $^{1}H$ and $^{13}C$, respectively), using a Bruker 5mm BBFO probe. Pulse widths were 14.1 and 10.5 μs for $^{1}H$ and $^{13}C$, respectively. All experiments were performed at room temperature. The $^{1}H$, $^{13}C$ decoupled from $^{1}H$, $^{1}H$-$^{13}C$ HSQC, $^{1}H$-$^{13}C$ HMBC, $^{1}H$-$^{1}H$ ROESY and $^{1}H$ diffusion NMR experiments were run under standard conditions. For HMBC experiment, a 50 ms waiting period was used for the evolution of long-range coupling, and a value of 3.4 ms for the low-pass *J* filter. ROESY was run with a spin-lock of 100ms for mixing. And diffusion measurements were done using standard stimulated echoes with bipolar gradient pulses, with $\Delta$ 300ms, $\delta$ 2.3ms, and 64 points for linear increment of the gradient between 0.96 and 47.2 $G.cm^{-1}$.

222 2.2.9. Structural characterization of the oxidation products

223 2.2.8.1. Separation and purification of oxidation products

224 Separation and fractionation of the oxidation products (OXP) solubilized in ultrapure
225 water were performed using high-performance semi-preparative liquid chromatography
226 (Gilson Inc., Middleton, USA). Results were processed using the Trilution @ LC software.
227 The OXP separation was carried out using a reversed-phase column GRACE Apollo C18 (250
228 x 22 mm - 5 µm). The detection was carried out at 322 nm on a UV/Vis 156 detector. The
229 elution gradient consisted in a phase A (ultra-pure water and formic acid 100: 0.1) and a phase
230 B (acetonitrile and formic acid 100: 0.1) at a flow rate of 10 $mL.min^{-1}$. 1 mL of sample was
231 injected into the column at a concentration of 4% w/v. The gradient consisted in 10% of the
232 phase B for 2 min, then 60% for 78 min, 99% for 5 min and finally 10% for 5 min. Fractions
233 were recovered from the column outlet in glass tubes. The solvents were evaporated using a
234 rotary evaporator BUCHI R144 (BUCHI SARL, Rungis, France). The OXP were freeze-dried
235 and then stored at 4 °C in a desiccator until use.

236 2.2.8.2. Determination of the molecular mass of the oxidation products by Liquid
237 Chromatography-Mass Spectrometry (LC-MS/MS)

238 The mass spectra of the OXP were obtained with a UHPLC-MS system, which
239 comprised a quaternary solvent delivery pump connected to a photodiode array and a LTQ
240 Orbitrap hybrid mass spectrometer (Thermo Fisher Scientific, San Jose, CA, USA) equipped
241 with an atmospheric pressure ionization interface operating in electrospray mode (ESI).

242 10 µl of the mixture were separated on a C18 Alltima (150 * 4.6 mm – 5µm) column
243 (Grace/Alltech, Darmstadt, Germany). The flow rate was set at 200 $µl.min^{-1}$ and mobile

phases consisted in water modified with formic acid (0.1%) for A and acetonitrile modified with formic acid (0.1%) for B. Phenolic compounds were eluted using a linear gradient from 5% to 47% of B for 60 min.

The spray voltage was +5.0 kV. The temperature of the heated capillary was set to 300 °C. The flow rates of sheath gas, auxiliary gas, and sweep gas were set (in arbitrary units/min) to 40, 10, and 10, respectively. Capillary voltage was +36 V, tube lens was +80 V, split lens was -44 V, and the front lens was -3.25 V. Mass spectrometric parameters were optimized by infusing a standard solution of isopimpinelline (0.1 $g.L^{-1}$) in mobile phase at a flow rate of 5 $\mu l.min^{-1}$. Parent ions were detected between 100 and 1000 m/z and specific $MS^n$ fragmentation spectra ($MS^2$, $MS^3$) were carried out in order to obtain structural information on OXP. Data were processed using Xcalibur software (version 2.1, Thermoscientific).

2.2.8.3. Nuclear magnetic resonance analyses

OXP were characterized by NMR according to the same method described for NGA and FGA. The only difference was the solvent and concentration used which in this case were a deuterated water/deuterated methanol mixture (50: 50) at a concentration of 20 mM. The structure determination was done using $^1H$, J-modulated $^{13}C$, $^1H$-$^1H$ COSY, $^1H$-$^{13}C$ HSQC, $^1H$-$^{13}C$ HSQC-TOCSY, and $^1H$-$^{13}C$ HMBC.

2.2.8.4. Size-exclusion chromatography coupled to multi-detectors

SEC experiments were performed with a HPLC pump (LC10AD, Shimadzu) coupled to an autosampler (Autosampler VE 2001, Malvern Panalytical) and a multi-detectors system recording UV, light scattering (RALS/LALS,) intrinsic viscosity and refractive index signals (Viscotek TDA305, Malvern Panalytical). Two SEC columns (A4000-A6000, 10 or 13 µm, 8

mm ID x 300 mm, void volume ~6 mL, total volume ~ 12.5 mL, Malvern Panalytical) were mounted in series and equipped with a post-column nylon filter (0.22 µm). The columns were equilibrated with ammonium acetate buffer 350 mM, pH 5.5. The flow rate was 0.35 mL.min$^{-1}$ and the temperature was 30 °C. Data were processed with the Omnisec software (v5.12, Malvern Panalytical). The calibration procedure was done with β-lactoglobulin (Sigma) and cross-validations were performed with PEO24k and Dextran standards (Viscotek PolyCal standards, Malvern Panalytical). The refractometer was used as the concentration detector and the refractive index increment value (dn/dc) used to determine the molecular weight was 0.136 mL/g (Grein *et al.*, 2013). Free-dried dialyzed samples were solubilized in the aforementioned buffer at 10 g.L$^{-1}$ and filtered through a 0.22 µm PES-filter just before injection.

## 3. Results and discussion

### 3.1. Color modification during the reaction

The first event that reflected a significant change during the oxidation of ferulic acid (FA) was a color change from colorless to dark red (pictures from Figure S1). Indeed, it was already shown in a previous study (Aljawish *et al.*, 2014) that the oxidation products of ferulic acid (OXP) were generally colored. Other polymers grafted with ferulic acid oxidation products were gradually modified towards yellow–orange during functionalization (Aljawish *et al.*, 2014; Karaki *et al.*, 2017). On Figure S1, the color difference of the reaction medium during the oxidation reaction of ferulic acid at different time are presented with and without GA. At this stage, it was important to evidence if the presence of GA modify the oxidation process. FGA and OXP color difference (ΔE, between t0, the beginning of the reaction and a

289 chosen time t) increased upon time, meaning that changes occurred from the beginning of the
290 reaction until its end (50 min). The values of color difference of FGA were significantly
291 different when compared with those of OXP. The color change was more pronounced without
292 GA (OXP). The 2 hypotheses formulated to explain this difference in coloring would be, on
293 one hand, the presence of GA and, on the other hand, a slightly lower level of oligomerization
294 in the presence of GA which blocks certain reaction intermediates by grafting. For the first
295 hypothesis, GA was not soluble in the buffer (heterogeneous catalysis), so the presence of the
296 polymer could have made the mixture a little turbid, thus changing the color parameters.
297 However, the tendencies were close, which could indicate that the oxidation products were
298 most probably the same with or without GA.

299

300 3.2. Monitoring of the ferulic acid consumption during the reaction

301 In order to verify if GA did not change the laccase activity or the ferulic acid
302 consumption rate, the consumption of ferulic acid in the reaction mixtures was monitored by
303 HPLC throughout the oxidation process.

304

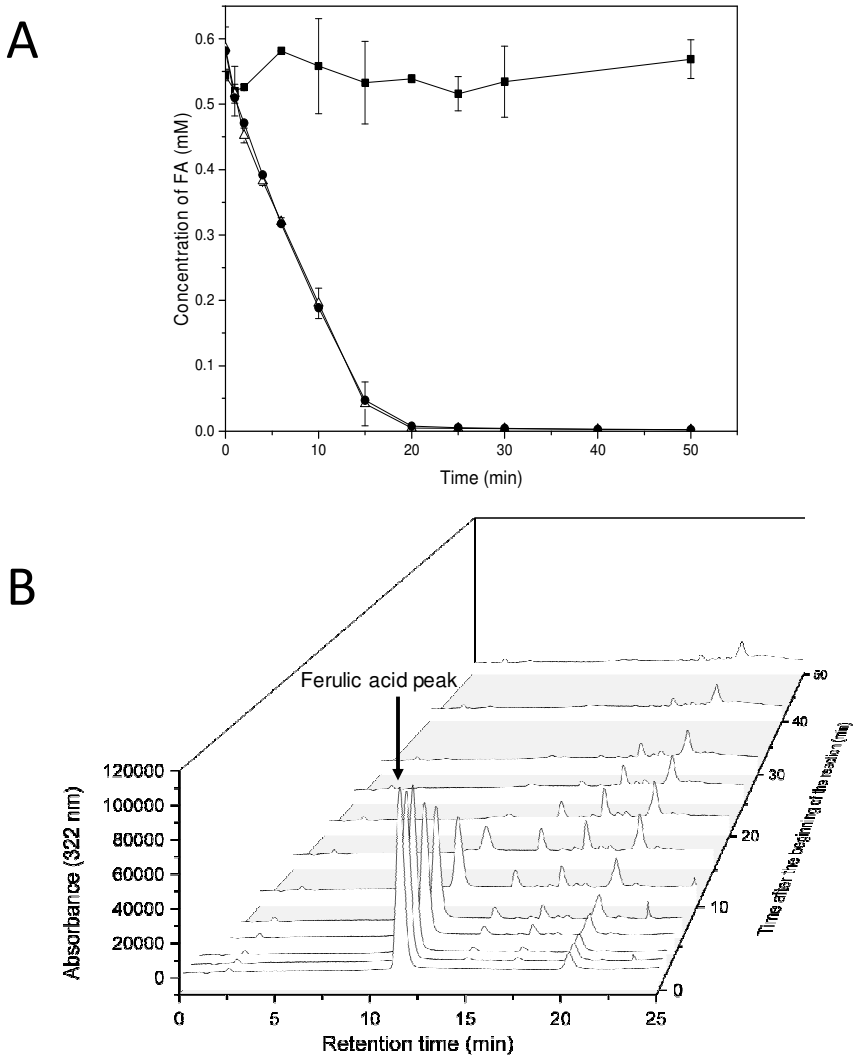


Figure 1: (A) Ferulic acid (FA) concentration in phosphate buffer (50 mM, pH 7.4, 30 °C) containing ferulic acid + gum Arabic + laccase (Δ), ferulic acid + laccase without gum Arabic (●) and ferulic acid + gum Arabic without laccase (control) (■) and (B) Chromatogram at 322 nm of the oxidation products of ferulic acid at different reaction times, from the beginning of the reaction to the end of the reaction (50 min).

The consumption of ferulic acid during the reaction with or without GA was monitored by assaying its disappearance from HPLC chromatograms at 322 nm (Figure 1). A control was made with GA and ferulic acid without laccase to ensure the FA concentration would not

316 decrease without laccase, i.e. that FA did not adsorb onto or react with GA. The results
317 presented on Figure 1.A indeed confirmed that FA concentration did not decrease upon time
318 without the enzyme. Physicochemical interactions between phenolic acids and
319 polysaccharides have already been observed by other authors (Padayachee *et al.*, 2012), but in
320 this case, the assumption that ferulic acid would adsorb onto GA chains was ruled out.
321 However, when laccase was added, the FA concentration decreased rapidly and similarly with
322 or without GA (0.52 ± 0.01 mM $FA.min^{-1}$ for OXP and 0.52 ± 0.02 mM $AF.min^{-1}$ for FGA).
323 These results suggested that the presence of GA did not interfere with the laccase activity and
324 did not affect the reaction rate. Some authors have reported the rate of reaction of phenol
325 substrate would be slowed down by adding a polymer (Karaki *et al.*, 2017; Sun, Payne, Moas,
326 Chu, & Wallace, 1992; Wada, Ichikawa, & Tatsumi, 1993) but another study on
327 polysaccharide functionalization (Aljawish *et al.*, 2012), also performed under heterogeneous
328 catalysis, demonstrated that the presence of the polymer would not change the reaction rate.

329 On Figure 1A it can be observed that almost all ferulic acid was consummated after 20
330 min (0.005 ± 0.001 mM remained for OXP and 0.002 ± 0.001 mM for FGA). This result was
331 quite surprising because the color of the reaction still evolved between 20 and 50 min for both
332 reactions (Figure S1). This could be explained by the reaction pathway. Laccase oxidized
333 phenols in *ortho* or *para* position into quinones and semi-quinones (Witayakran & Ragauskas,
334 2009) that were unstable and could then react with other molecules. Once they are formed,
335 according to the resulting structure, the oxidation products can then react with another ferulic
336 acid molecules or other oxidation products or be oxidized once again by the enzyme.
337 Numerous structural changes may also occur, for example by oxidative decarboxylation, thus
338 increasing the number of possible structures grafted onto the polysaccharide (Aljawish *et al.*,
339 2012; Karaki *et al.*, 2016). In addition, these molecular reorganizations are often accompanied

by an increase in molecular mass leading to the appearance of more sustained colors, which is observed by colorimetry. In order to understand the changes that occurred after FA was consummated, and to follow the number of oxidation products formed and their modification upon time, the absorbance at 322 nm of the oxidation products of ferulic acid upon retention time, all along the reaction, was studied by HPLC. After the peak recorded at 11.4 min associated to ferulic acid (peak area used to follow its disappearance upon time) several other peaks appeared and may then sometimes disappeared related to the apparition or the disappearance of several oxidation products.

### 3.3.Study of the oxidation products

The absorbance at 322 nm of the mixtures (Figure 1.B) revealed the presence of several peaks that corresponded to different oxidation products. Their retention times were higher than that of ferulic acid (11.4 min), meaning they were more hydrophobic related to the eluent composition. Some products were formed during the reaction but disappeared before the end (for example the peak at a retention time of 14.7 min). At the end of the reaction, a massive group of peaks was observed in the range of retention time from 17.0 to 21.1 min. The oxidation products did indeed change between 20 and 50 min of reaction, thus explaining why the color of the samples would change (Figure S1) even after all FA was consummated.

Each observed absorbance peaks corresponded to one oxidation product which might react with the polysaccharide when GA was present in the reaction media. Their structures were thus further investigated by LC-MS/MS.

Thanks to UV screening at 322nm recorded during more than 60 minutes, 11 oxidation products were readily identified by LC-MS/MS analysis 50 minutes after the enzyme addition as shown in Figure 2 giving their retention time and their exact molecular mass. The peak n°1

corresponded to dehydrated ferulic acid (shown by its molecular mass (177.06 g.mol$^{-1}$) and retention time (26 s)). The peak n°6 has a molecular mass close to the one of ferulic acid ($M_{FA}$=194.18 g.mol$^{-1}$) so it would seem, therefore, that it corresponded to a molecule with only one phenolic ring with a structure close to the one of ferulic acid. From their molecular weights, OXP n° 2 and 9 were most probably ferulic acid derivatives trimers formed with three derivatives of ferulic acid whereas the majority of the 7 other OXP were obviously ferulic acid derivatives dimers as already observed in previous studies (Aljawish *et al.*, 2014; Carunchio, Crescenzi, Girelli, Messina, & Tarola, 2001).

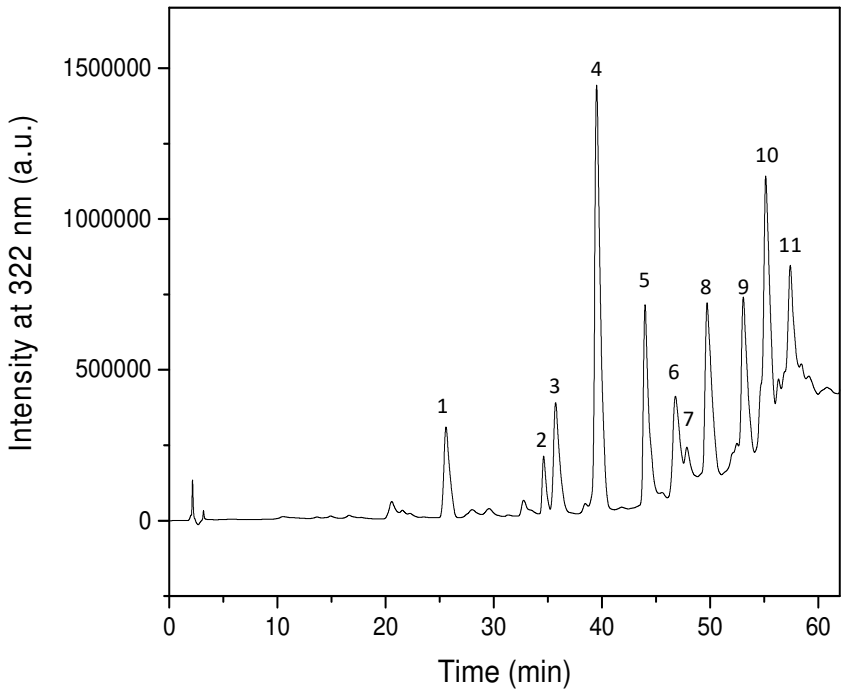


| Peak number | Exact molar mass (g.mol$^{-1}$) | Retention time (s) |
|---|---|---|
| 1 | 177.0574 | 26.245 |
| 2 | 609.1849 | 35.152 |
| 3 | 340.0946 | 36.292 |
| 4 | 386.1000 | 40.117 |
| 5 | 340.0945 | 44.513 |
| 6 | 200.0470 | 47.190 |
| 7 | 340.0945 | 48.821 |
| 8 | 342.1101 | 50.282 |
| 9 | 588.1608 | 53.572 |
| 10 | 340.0944 | 57.848 |
| 11 | 340.0944 | 59.311 |

Figure 2: Absorbance at 322 nm and retention time of the oxidation products of ferulic acid (at the end of the reaction) and corresponding molecular exact mass (precise until $10^{-4}$ g.mol$^{-1}$).

In order to investigate further their structure, the OXP were fractionated using high-performance semi-preparative liquid chromatography. Based on the purity and quantity of the

377 OXP obtained for each peak, further LC-MS/MS and NMR investigations were performed
378 only on OXP n° 3, 4, 5, 8 and 9.

379 The chosen OXP were analyzed by LC-MS/MS. From the exact molecular mass, formula
380 predictions were generated. The most probable formula prediction (the one for which the
381 exact mass was closest to the one measured) was presented in Table 1, along with neutral
382 losses identified in $MS^2$ and $MS^3$ spectra. These OXP were also analyzed by NMR ($^1H$ and
383 $^{13}C$ measurements). Due to problems of concentration and thus NMR sensitivity issues, it was
384 not possible to fully elucidate the structure of all studied OXP. Information obtained from
385 standard NMR measurements ($^1H$ and $^{13}C$ measurements) are presented in supplementary
386 material (Table S1).

387 Table 1: Peak number from Figure 2, neutral losses from $MS^2$ and $MS^3$ spectra, most probable
388 formula prediction.

| Peak number | Exact mass | Most probable formula prediction | Neutral loss ($MS^2$) | Neutral loss ($MS^3$) |
|---|---|---|---|---|
| 3 | 340.0945 | $C_{19}H_{16}O_6$ | $CO_2$ | $CH_3OH$ |
| 4 | 386.1000 | $C_{20}H_{18}O_8$ | $CO_2$ | $H_2O$ |
| 5 | 340.0945 | $C_{19}H_{16}O_6$ | CO | $H_2O$ |
| 8 | 342.1101 | $C_{19}H_{17}O_6$ | $2H_2O$ | None |
| 9 | 588.1608 | $C_{32}H_{28}O_{11}$ | M=386 $g.mol^{-1}$ = OXP 4 | None |

389

390 This preliminary study revealed four of these five OXP were ferulic acid derivatives dimers
391 which probably kept their aromatic rings along with their methoxy groups. The fragmentation
392 of the OXP n° 9 revealed it was probably a trimer composed of a dimer similar to OXP n° 4

393 and another ferulic acid derivative. Another interesting result was the OXP fragmentations
394 were different, even for the ones with the same molecular mass (n° 3 and 5). These OXP had
395 different retention times (Figure 2), meaning their hydrophobia was different. Though the
396 most probable formulas for these products were the same, it would be difficult to presume to
397 design their structure solely based on their molecular mass, however this approach is often
398 available in literature.

399 From these results, it was admitted that most oxidation products were ferulic acid
400 derivatives dimers with two aromatic rings and methoxy groups onto it, meaning the most of
401 the oxidation product mechanism would involve forming ester bound between ferulic acids
402 carboxyl groups and hydroxyl groups (Table S1). Further NMR experiments were conducted
403 on the OXP n° 3 to clarify its structure.

404 3.4. Determination of the structure of the oxidation product n° 3

405 Since it was the one with the highest signal/noise ratio in $^{1}H$ and $^{13}C$ measurements, the
406 structure of the OXP 3 was investigated further.

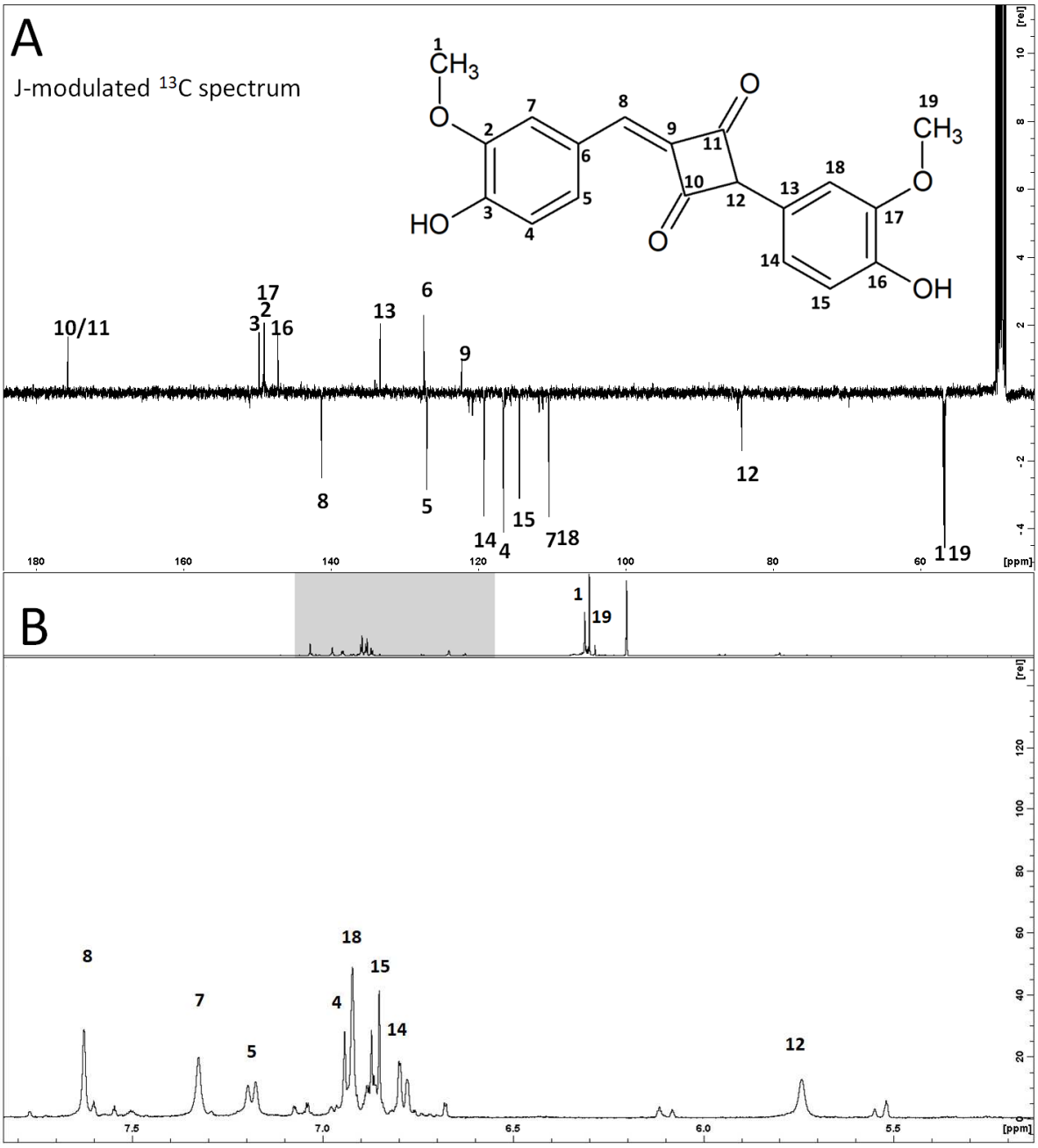


Figure 3: $^{13}C$ (A) and $^{1}H$ (B) spectra of the OXP n°3 (cyclobutadiferulone) (9.4T, ambient temperature, solvent $D_2O$/deuterated methanol) with the peaks' attribution (the chemical shift, J-coupling and $^{1}H$-$^{1}H$ COSY and $^{1}H$-$^{13}C$ HSQC spectra of the OXP n°3 are presented in supplementary material)

$^{13}C$ spectrum of the OXP n°3 is presented on Figure 3.A. It showed the presence of 18 signals. However, the predicted formula obtained from the molecular mass of the compound

415 contained 19 C (Table 1), which meant that two carbons were probably equivalent. $^{1}H$
416 spectrum of the OXP n°3 was presented on Figure 3.B and $^{1}H$-$^{1}H$ COSY experiment is
417 presented in supplementary materials (Figure S2). The characteristic signals for methoxy
418 groups were displayed at 3.88 and 3.82 ppm. The compound spectrum also showed six
419 aromatic proton at 6.91 (d; J=8 Hz), 6.84 (d; J=8 Hz), 7.17 (dd; J=8 and 1.7 Hz), 6.77 (dd; J=8
420 and 1.5 Hz), 7.31 (d; J=1.7 Hz) and 6.90 (d; J=1.5 Hz), characteristics for the H-4, H-15, H-5,
421 H-14, H-7 and H-18 of aromatic part of the compound. All chemical shifts and J-couplings
422 are presented in supplementary materials (Table S2) These results, along with the knowledge
423 of the substrate peaks attributions (Sajjadi *et al.*, 2012) led to presume there were two
424 aromatic rings from ferulic acid with the methoxy and the hydroxy groups on them.
425 Correlations obtained by $^{1}H$-$^{13}C$ HSQC and $^{1}H$-$^{13}C$ HMBC measurements confirmed this
426 hypothesis and are presented in supplementary materials (Figure S3). Only one peak was
427 observed in the aldehyde/ketone area of the carbon-13 spectrum (175.7 ppm) leading to the
428 assumption there were C=O equivalent groups. They were both correlated to the proton in C-
429 8. This OXP was then identified to be 2-(4-hydroxy-3-methoxyphenyl)-4-[(4-hydroxy-3-
430 methoxyphenyl) methylidene] cyclobutane-1, 3-dione presented on Figure 3, called by the
431 authors cyclobutadiferulone. This molecule possesses a tautomeric form that could potentially
432 be charged in solution (Figure S4), but in NMR measurement only one form was detected. It
433 was not possible to propose a mechanism for this OXP formation, which suggested that it did
434 not result simply from the reaction of two oxidized ferulic acids derivatives. The most
435 probable hypothesis was that one ferulic acid was first oxidized/modified by the enzyme and
436 that this intermediate product would have reacted onto another ferulic acid molecule or a
437 modified one. In order to propose a mechanism for the 2-(4-hydroxy-3-methoxyphenyl)-4-[(4-
438 hydroxy-3-methoxyphenyl) methylidene] cyclobutane-1, 3-dione formation, further

investigations of the intermediate products that appear and then disappear during the reaction (Figure 1) have to be performed all along the reaction.

However, GA has several sites which may react with the oxidation products previously studied. The OXP could react with these functional groups to be covalently linked to the polysaccharide. The grafting of these products onto GA was thus investigated.

### 3.5. Modification of gum Arabic

The impact of OXP grafting on the molecular weight and hydrodynamic radius of GA has been determined using Size exclusion chromatography (SEC) coupled to a multi-detectors system (UV, LS, IV and RI signals were recorded). NGA was analyzed (Figure 4A) and three peaks were observed, corresponding to the expected GP, AGP and AG fractions (Picton *et al.*, 2000). The proportion of each fraction was determined using RI detector (0.7%, 10.6% and 88.7%, respectively). The determination of *Mw* using light scattering gave *Mw* of ~3.88 x $10^6$ $g.mol^{-1}$, ~1.25 x $10^6$ $g.mol^{-1}$ and ~3.33 x $10^5$ $g.mol^{-1}$ for the respective fractions. Finally, the determination of the hydrodynamic radius (*Rh*) was performed thanks to IV detector, giving values of ~28.2, 18.4 and 8.4 nm (see Table S1 in supporting information for a summary of the derived parameters). It is worth notifying that since no significant UV signal at 280 nm was observed, the determination or estimation of the protein content of each fraction was not possible. Nevertheless, all aforementioned results are in line with the literature (Randall *et al.*, 1989; Sanchez *et al.*, 2008).

460 FGA was analyzed in the same way (Figure 4B). The first observation was the
461 disappearance of the peaks corresponding presumably to the GP and AGP fractions. Indeed,
462 only one peak having a retention volume really close to the one of the AG fractions in NGA
463 was observed. It was concluded that the two fractions were eliminated during ethanol
464 precipitation realized after the enzymatic reaction leaving only a purified and functionalized
465 AG fraction. *Mw* obtained for NGA was ~2.13 x $10^5$ g.mol$^{-1}$ and *Rh* was 6.6 nm (see Table S3
466 for a summary of the derived parameters). Such values indicated that a large decrease of *Mw*
467 of the AG fraction occurred during the purification process and/or that a sub-fraction of AG
468 was purified that was previously observed by HIC purification (Atgié *et al.*, 2019).
469 Surprisingly, no UV signal at 322 nm was observed, certainly due to the small amount of
470 OXP present on FGA. It was also observed that after filtration through 0.22 PES filter just
471 before injection, the sample was colorless and no longer orange. Interestingly, the nylon post-
472 column filter was yellowish after unmounting meaning again that excess of OXP. Excess of
473 unbound OXP could have been stuck onto the filters. Nevertheless, thanks to the purification
474 procedure of FGA, a purified and likely functionalized fraction was isolated, having a
475 remarkably small polydispersity index of ~1.04 (Table S3).

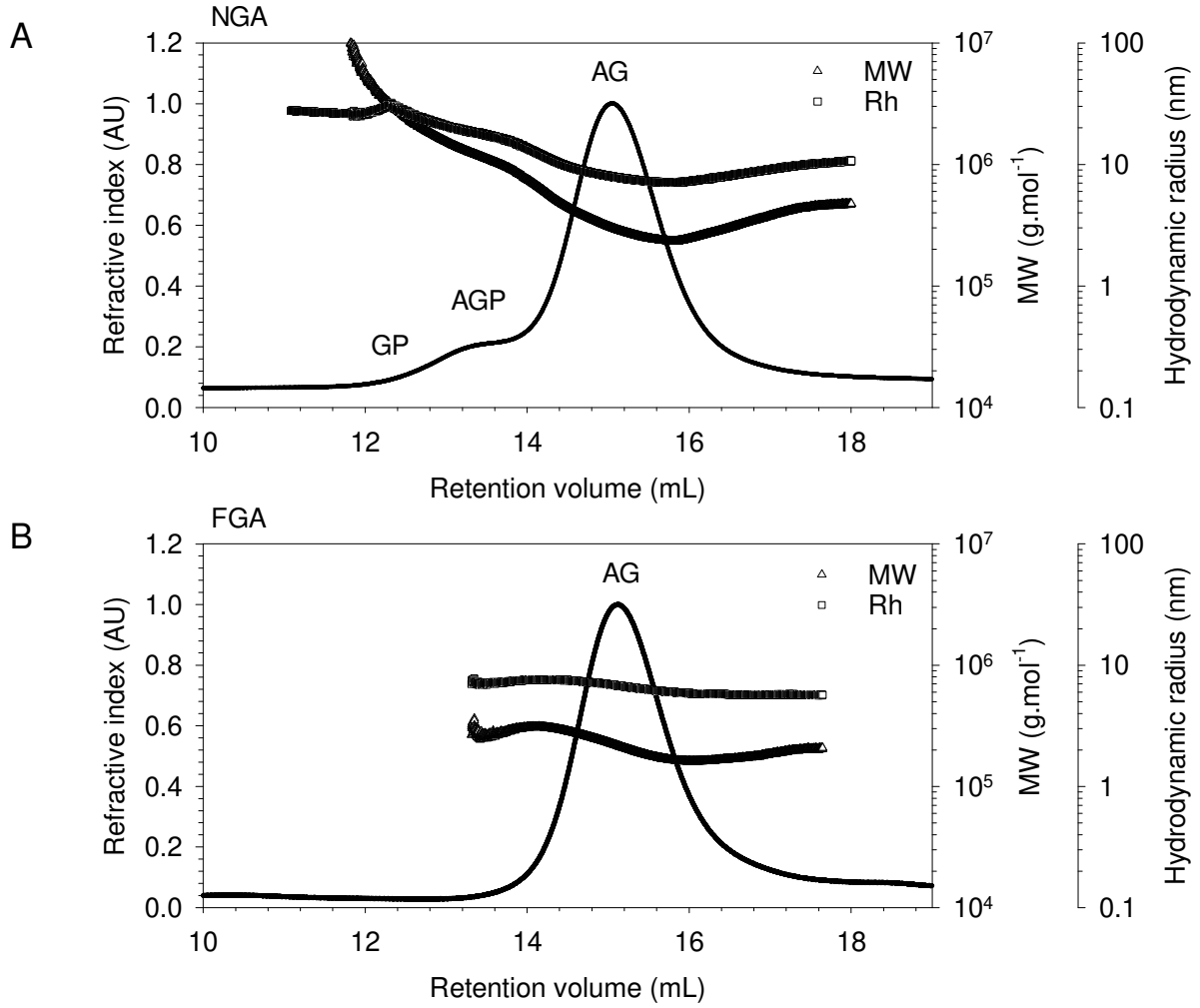


476

477 Figure 4: Size exclusion chromatography characterization (refractive index in filled line, $M_w$
478 Δ, Rh □) of native gum Arabic (NGA) (A) and functionalized gum Arabic (FGA) (B). AG =
479 arabinogalactan-peptide, AGP = arabinogalactan protein and GP = glycoprotein.

480

481 It was seen previously that the studied OXP could be charged in solution. Several
482 authors already studied the ferulic acid oxidation products molecular mass and suggested that
483 they would be mostly negatively charged dimers of ferulic acid (Adelakun *et al.*, 2012;
484 Aljawish *et al.*, 2014). If they were grafted onto GA, it should change its charge.
485 Furthermore, the FGA being a functionalized AG fraction, it should contain less amine groups

and more uronic acid groups, which is responsible for its negative charge. This should lead to FGA charge being lower than NGA charge in solution (Grein-Iankovski et al., 2018).

The Approximate Zeta potentials of NGA and FGA in ultrapure water were measured at pH 5.5, 25 °C, at 1 % w/v. At this pH, the uronic groups of NGA and FGA should be deprotonated (pKa of 3.6, (Aberkane et al., 2010)) as well as grafted ferulic acid oxidation products (pKa aroud 4.6 (Dempsey et al., 1979)) and the amine groups on NGA should be protonated ($pKa_2$ around 6.5 (Grein-Iankovski et al., 2018)).

The NGA Approximate Zeta potential was -25.8 + 0.6 mV, which was related to the presence of the carboxylic groups of the glucuronic acid. This value decreased to -30.1 + 0.9 mV when GA was functionalized, as it was expected from the absence of the GP and AGP fractions in FGA.

The decrease of the charge (or the increase of the negative charge) of GA after functionalization was the first hint that the oxidation products were grafted onto it, however it was not possible to make hypothesis on where it was grafted. They could possibly be grafted onto amino groups of the proteinaceous fraction by forming a Schiff base bound as for chitosan (Aljawish *et al.*, 2012) or onto carboxyl groups of the glucuronic acids by forming an ester as for pectin (Karaki *et al.*, 2017). The negative charge of GA was expected to be stable or to increase after functionalization, whether they replace a carboxylic charge or an amine charge.

Zeta Potential measurements and SEC-MALS analysis evidenced a strong modification of GA by the enzymatic functionalization process attributed to the grafting of ferulic acid derivatives.

508 Therefore, Nuclear Magnetic Resonance (NMR) was used in order to get better insight of the
509 location of the grafting onto GA.

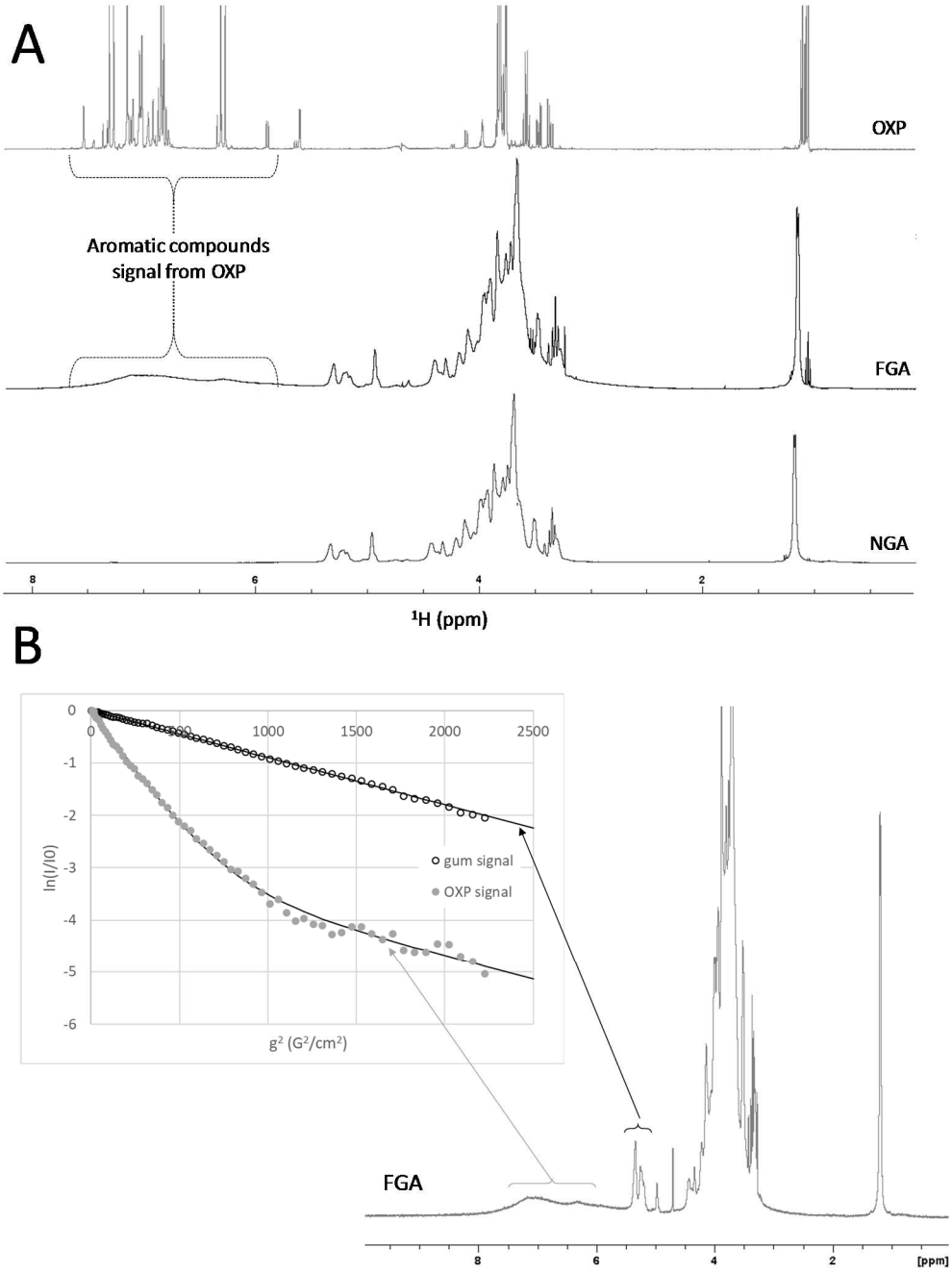


510

511

512 Figure 5: (A) $^{1}$H NMR spectra of oxidation products (OXP), functionalized gum Arabic
513 (FGA) and native gum Arabic (NGA) and (B) $^{1}$H NMR spectra of functionalized gum Arabic
514 (FGA). In the inset: evolution of the signal (logarithmic scale, as a function of the gradient g
515 applied) obtained by pulsed field gradient measurement, for two different areas of the spectra.
516 (•) Signal of OXP from 6.0 to 7.5 ppm; (○) signal of gum Arabic from 5.0 to 5.5 ppm. The
517 diffusion coefficients were obtained from these evolutions.

518

519 $^{1}$H NMR experiments were performed on three samples: NGA, FGA and OXP (Figure 5.A).
520 The signals of NGA and FGA were crowded between 3.0 and 6.0 ppm, which is typical of
521 polysaccharides and reflected the presence of the sugar residues (Nie *et al.*, 2013). Those
522 signals have not been deteriorated after functionalization, meaning that the polymer main
523 structure was preserved. On the OXP spectrum, the peaks between 6.0 and 7.5 ppm were
524 characteristic of aromatic proton (Sajjadi, Shokoohinia, & Moayedi, 2012). On the spectrum
525 of dialyzed FGA, broad signals were visible in this aromatic compound area (6.0 to 7.5 ppm),
526 which corresponded to the grafted OXP. The signal was not very intense due to the weak
527 grafting rate and to the broadening due to the loss of mobility occurring in the grafting.

528 Pulsed field gradient (PFG) is a common NMR technique to study the diffusion of polymers
529 (Callaghan & Pinder, 1985; Dixon & Larive, 1997; Oostwal, Blees, de Bleijser, & Leyte,
530 1993). Such measurement was made on the NGA and FGA samples (Figure 5.B).

531 NGA was found to have a unique diffusion coefficient (around 1 x $10^{-11}$ $m^2.s^{-1}$, data not
532 shown). Results obtained on the FGA sample (Figure 5.B) were analyzed considering two
533 distinct areas of the $^{1}$H one-dimensional NMR spectrum. In the area corresponding to the gum
534 signal only (between 5.0 and 5.5 ppm), a unique diffusion coefficient was obtained, as shown
535 by signal monotonous evolution obtained in the inset of Figure 5.B (open symbols). The
536 obtained value of 2 x $10^{-11}$ $m^2.s^{-1}$, slightly higher than the one obtained with NGA, indicated a
537 decrease of the polymer size and/or a decrease in medium viscosity after functionalization.
538 The evolution of the hydrodynamic radius determined from the diffusion coefficient using the
539 Stockes-Einstein equation (Gaylord and Gibbs, 1962) are in good correlation with the ones
540 obtained from SEC-multi-detectors experiments (Table S1). Indeed, the calculated R*h* based
541 on the diffusion coefficient (21.8 nm for NGA and 10.9 nm for FGA) showed the same

542 tendency as the ones obtained from SEC- multi-detectors experiments (9.6 nm for NGA and
543 6.6 nm for FGA). In both cases, the polymer size decreased after functionalization. The
544 different values of hydrodynamic radius may be the result of the experiment being performed
545 in different solvents. Indeed, the $R_h$ can vary in a given solvent because of its ability to
546 increase and expand the polysaccharide coils (Antoniou *et al.*, 2010).

547 Furthermore, in the area corresponding to OXP signals (6.0 to 7.5 ppm) on the FGA spectrum,
548 two diffusion coefficients were obtained, as indicated by the slope break on the inset of Figure
549 5.B (filled symbols). These two coefficients indicated that there were two types of OXP. One
550 of the diffusion coefficients was the same as the one of the gum signal of FGA ($2 \times 10^{-11}$ $m^2.s^-$
551 $^1$, parallel lines between gum and OXP signals from 1000 to 2500 $G^2.cm^{-2}$ in the diffusion
552 experiment) and could therefore be attributed to a fraction of OXP linked to the gum. The
553 other coefficient was faster (around $8 \times 10^{-11}$ $m^2.s^{-1}$) and could be attributed to a fraction of
554 OXP that were not directly linked to the functionalized GA. This fraction could correspond to
555 a small fraction of non-grafted oxidation products that were not eliminated during dialysis
556 because they were strongly adsorbed on FGA. Diffusion measurements could thus show that a
557 fraction of OXP was grafted onto FGA, 2D NMR approaches were then performed in order to
558 locate were they were grafted.

559 HMBC spectra were obtained on the three samples. These spectra were first used in order to
560 obtain information on the carboxyl zone before and after functionalization. Indeed, a direct
561 $^{13}C$ measurement was not conceivable because of a lack of sensitivity, indirectly detected $^{13}C$
562 spectra (using $^1H$ polarization) of the three samples were thus obtained from projections of the
563 HMBC (Figure 6). It appeared on these spectra the additional peaks observed on the
564 functionalized gum corresponded to phenolic groups signals. In a second step, and in order to
565 verify if there was a correlation between the FGA carbons and the protons from OXP, HMBC

566 correlation were finely analyzed (supplementary material, Figure S5). The weak proportions
567 of OXP did not make it possible to visualize a direct correlation between the aromatic $^{1}H$ of
568 OXP and a carbon of FGA. Even if only intra-OXP or intra-gum correlations could be
569 observed in the HMBC, carboxyl carbon peak moved from 175.4 ppm in the OXP mixture to
570 168.2 ppm in the FGA sample, which may indicate that OXP were possibly esterified.

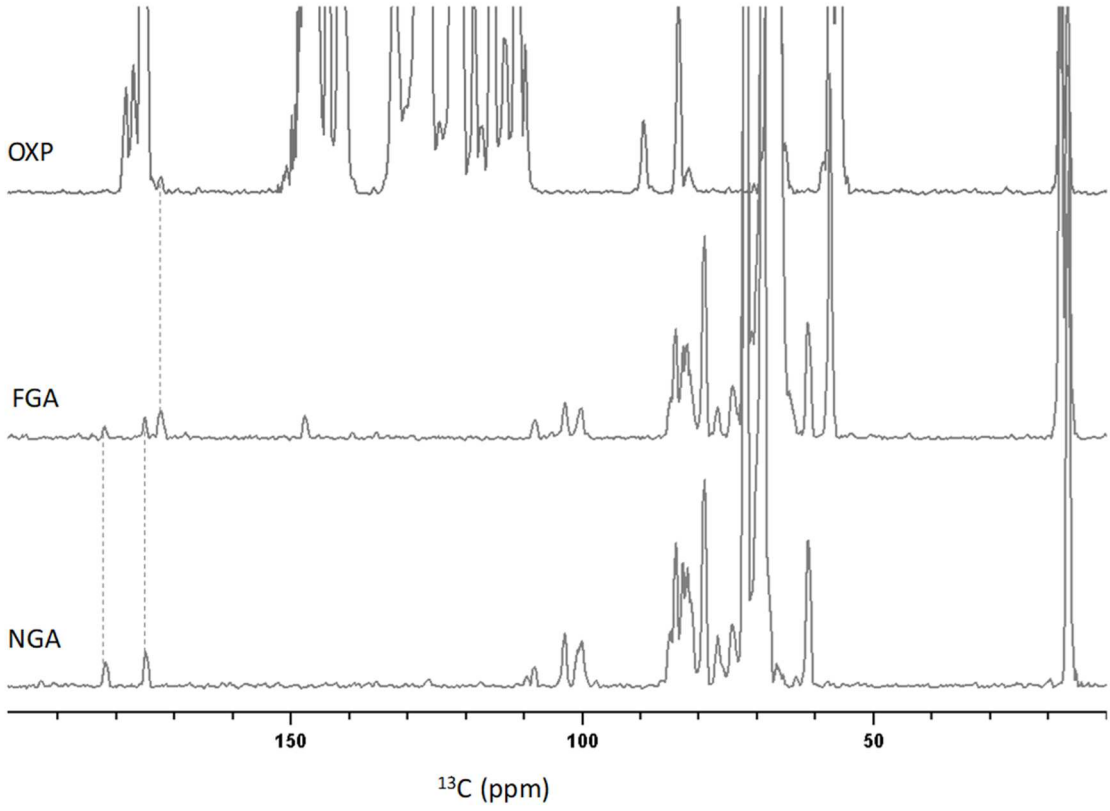


571

572 Figure 6: $^{13}C$ NMR spectra obtained from the projections of HMBC recorded on oxidation
573 products (OXP), native gum Arabic (NGA) and functionalized gum Arabic (FGA).

574 ROESY experiments of FGA were recorded (Figure 7). They allowed the visualization of a
575 $^{1}H$-$^{1}H$ correlation by dipolar effect and thus drove to identify protons that were close in space.
576 A $^{1}H$-$^{1}H$ dipolar interaction was visible between the aromatic $^{1}H$ of OXP and GA but it was
577 difficult to clearly identify the corresponding $^{1}H$ due to the width of the correlation spots and
578 their low intensity. However, a correlation was brought out between one aromatic $^{1}H$ of OXP

579 and possibly the methylic protons of FGA galactose units (in C6) or the $^{1}H$ in C5 of the
580 glucuronic acid units of GA, meaning the OXP would be grafted either onto them or onto the
581 near carbons. The results obtained in a previous study on pectin modification by grafting OXP
582 of ferulic acid (Karaki *et al.*, 2017) with the same pathway also concluded on a grafting onto
583 the C6 carbon of the galacturonate units of pectin.

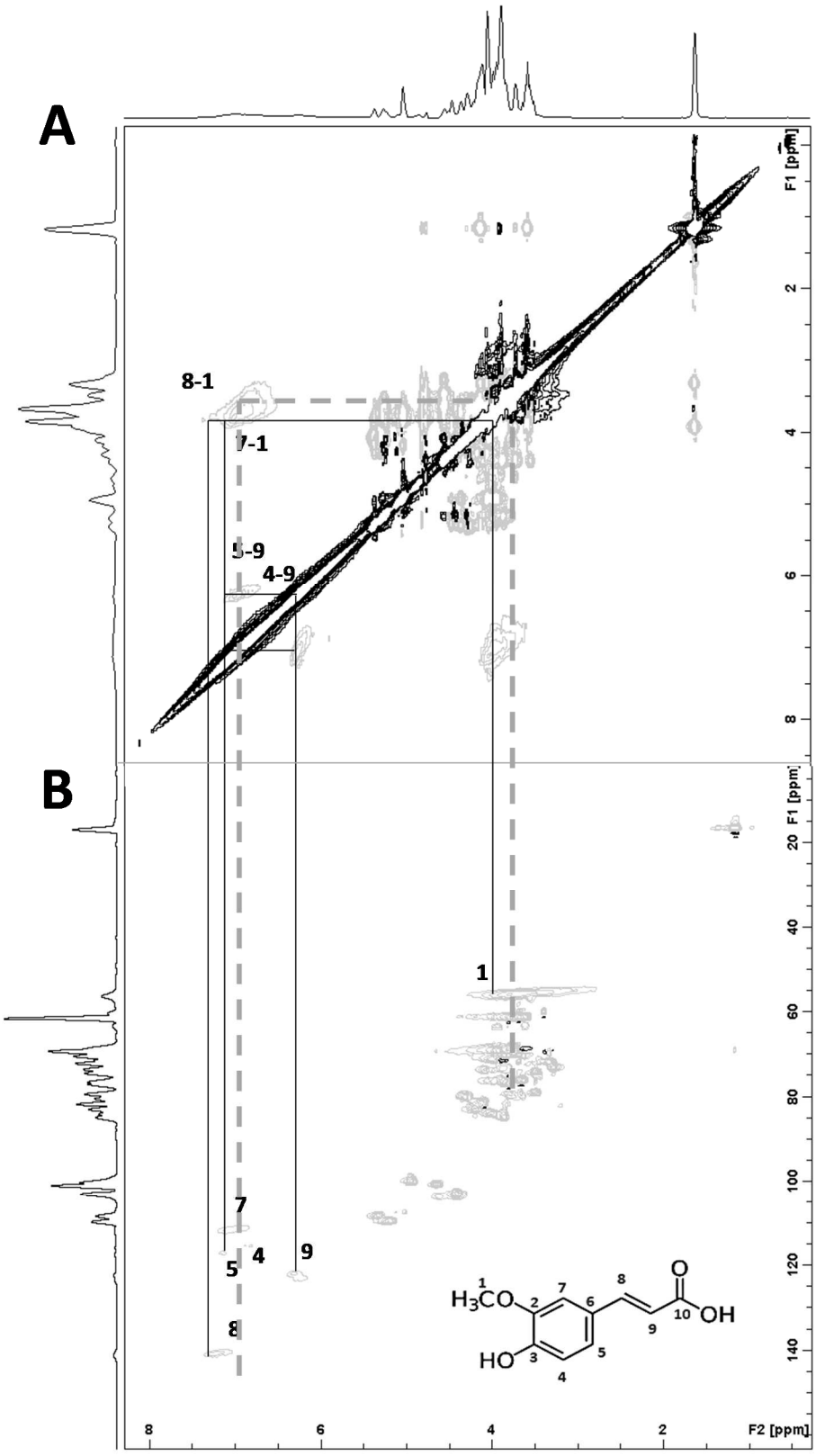


584
585 Figure 7: (A) ROESY $^{1}H$-$^{1}H$ and (B) HSQC $^{1}H$-$^{13}C$ of functionalized gum Arabic FGA. As a
586 reference for OXP, the signals corresponding to ferulic acid are indicated according to the

numbering of the figure in the inset of (B). Intra-OXP correlations are indicated by straight lines. Gum Arabic-OXP correlation is indicated by a dotted line.

To summarize, the pulsed field gradient (PFG) measurements indicated that after dialyses there were still two populations of OXP in solution. One of them could be referred to as "free OXP" and the other one was strongly bound to FGA. Nevertheless, the presence of a chemical bonding between OXP and FGA was not obvious by experimental 2D NMR, due to the complexity of the spectra and especially sensitivity problems because of the low grafting rate of OXP. However, there was a set of clues proving that the grafting was conclusive, the strongest one being that the diffusion coefficient of GA was modified after functionalization and this coefficient was also measured in the spectral area corresponding to the OXP species. Although, no direct interaction between OXP and GA could be evidenced by HMBC. ROESY correlations proved the proximity of both compounds and made it possible to estimate a location for the site of the grafting: close to the C6 of galactose units or close to the C5 of the glucuronic acid units of GA, which was consistent with what was observed on other polymers (Karaki *et al.*, 2017).

## 4. Conclusions

This study focused on the modification of gum Arabic by an enzymatic pathway. The first result was that GA did not alter the enzymatic oxidation of ferulic compounds since neither the color nor the ferulic acid consumption were modify in the presence of the polysaccharide. Furthermore, it was observed by HPLC that several oxidation products were formed which may then react with GA. The exact mass of each OXP was determined by LC-MS/MS, leading to the conclusion that the majority of the products obtained were ferulic acid

610 dimers which kept their aromatic rings and the O-$CH_3$ groups onto them. Assumptions were
611 made about their respective raw formulas and one of them was clearly identified from NMR
612 experiments as cyclobutadiferulone (2-(4-hydroxy-3-methoxyphenyl)-4-[(4-hydroxy-3-
613 methoxyphenyl) methylidene] cyclobutane-1,3-dione). Further experiments will have to be
614 carried out in order to make it possible for all OXP structures to be elucidated and to propose
615 a mechanism for their formation. However, the grafting of oxidation products onto GA
616 modified its charge (its approximate Zeta potential decreased) and only one fraction was
617 recovered after functionalization instead of the three of the native gum. SEC-MALS analysis
618 indeed evidenced that only AG fraction remained but with lower molecular weight and
619 polydispersity. From NMR analysis, oxidation products were undeniably present on modified
620 GA, probably close to the glucuronic acid C5 carbon or close to the galactose C6 carbon. In
621 spite of the complexity of such a system due to the number and variability of the ferulic acid
622 oxidation products, the complexity of GA with its three fractions and its high polydispersity,
623 the combination of various well-chosen technics allowed the confirmation of the grafting of
624 ferulic acid derivative onto GA and a better knowledge on the laccase-assisted modification of
625 polysaccharide.

626

627 AUTHOR INFORMATION

628 Corresponding Author Email: jordane.jasniewski@univ-lorraine.fr

629 ACKNOWLEDGMENTS AND FUNDING

630 The authors acknowledge support of the LIBio by the "Impact Biomolecules" project of the
631 "Lorraine Université d'Excellence" (Investissements d'avenir – ANR).

We would like to thank Nexira for kindly providing the Gum Arabic used in this article.

We also thank Aurélie Seiler for the technical support and the Plateforme de RMN de l'Institut Jean Barriol, Université de Lorraine.

This research did not receive any specific grant from funding agencies in the public, commercial, or not-for-profit sectors.

REFERENCES

Aberkane, L., Jasniewski, J., Gaiani, C., Scher, J., & Sanchez, C. (2010). Thermodynamic characterization of acacia gum-beta-lactoglobulin complex coacervation. *Langmuir: The ACS Journal of Surfaces and Colloids*, *26*(15), 12523–12533. https://doi.org/10.1021/la100705d

Adelakun, O. E., Kudanga, T., Parker, A., Green, I. R., le Roes-Hill, M., & Burton, S. G. (2012). Laccase-catalyzed dimerization of ferulic acid amplifies antioxidant activity. *Journal of Molecular Catalysis B: Enzymatic*, *74*(1), 29–35. https://doi.org/10.1016/j.molcatb.2011.08.010

Aljawish, A., Chevalot, I., Jasniewski, J., Paris, C., Scher, J., & Muniglia, L. (2014). Laccase-catalysed oxidation of ferulic acid and ethyl ferulate in aqueous medium: A green procedure for the synthesis of new compounds. *Food Chemistry*, *145*, 1046–1054. https://doi.org/10.1016/j.foodchem.2013.07.119

Aljawish, A., Muniglia, L., Klouj, A., Jasniewski, J., Scher, J., & Desobry, S. (2016). Characterization of films based on enzymatically modified chitosan derivatives with

phenol compounds. *Food Hydrocolloids*, *60*, 551–558. https://doi.org/10.1016/j.foodhyd.2016.04.032

Aljawish, A., Chevalot, I., Piffaut, B., Rondeau-Mouro, C., Girardin, M., Jasniewski, J., Scher, J., Muniglia, L. (2012). Functionalization of chitosan by laccase-catalyzed oxidation of ferulic acid and ethyl ferulate under heterogeneous reaction conditions. *Carbohydrate Polymers*, *87*(1), 537–544. https://doi.org/10.1016/j.carbpol.2011.08.016

Antoniou, E., Buitrago, C. F., Tsianou, M., & Alexandridis, P. (2010). Solvent effects on polysaccharide conformation. *Carbohydrate Polymers*, *79*(2), 380–390. https://doi.org/10.1016/j.carbpol.2009.08.019

Atgié, M., Garrigues, J. C., Chennevière, A., Masbernat, O., & Roger, K. (2019). Gum Arabic in solution: Composition and multi-scale structures. *Food Hydrocolloids*, *91*, 319–330. https://doi.org/10.1016/j.foodhyd.2019.01.033

Berka, R. M., Schneider, P., Golightly, E. J., Brown, S. H., Madden, M., Brown, K. M., Mondorf, K., Xu, F. (1997). Characterization of the gene encoding an extracellular laccase of Myceliophthora thermophila and analysis of the recombinant enzyme expressed in Aspergillus oryzae. *Applied and Environmental Microbiology*, *63*(8), 3151–3157.

Callaghan, P. T., & Pinder, D. N. (1985). Influence of polydispersity on polymer self-diffusion measurements by pulsed field gradient nuclear magnetic resonance. *Macromolecules*, *18*(3), 373–379. https://doi.org/10.1021/ma00145a013

673 Carunchio, F., Crescenzi, C., Girelli, A. M., Messina, A., & Tarola, A. M. (2001). Oxidation
674 of ferulic acid by laccase: identification of the products and inhibitory effects of some
675 dipeptides. *Talanta*, *55*(1), 189–200. https://doi.org/10.1016/S0039-9140(01)00417-9

676 Dempsey, B., Serjeant, E. P., & International Union of Pure and Applied Chemistry (Eds.).
677 (1979). *Ionisation constants of organic acids in aqueous solution*. Pergamon Press.

678 Dixon, A. M., & Larive, C. K. (1997). Modified Pulsed-Field Gradient NMR Experiments for
679 Improved Selectivity in the Measurement of Diffusion Coefficients in Complex
680 Mixtures: Application to the Analysis of the Suwannee River Fulvic Acid. *Analytical*
681 *Chemistry*, *69*(11), 2122–2128. https://doi.org/10.1021/ac961300v

682 Espinosa-Andrews, H., Sandoval-Castilla, O., Vázquez-Torres, H., Vernon-Carter, E. J., &
683 Lobato-Calleros, C. (2010). Determination of the gum Arabic–chitosan interactions by
684 Fourier Transform Infrared Spectroscopy and characterization of the microstructure
685 and rheological features of their coacervates. *Carbohydrate Polymers*, *79*(3), 541–546.
686 https://doi.org/10.1016/j.carbpol.2009.08.040

687 Gaylord, N.G., Gibbs, J.H. (1962). Physical chemistry of macromolecules. C. Tanford. Wiley,
688 New York, 1961. *Journal of Polymer Science, 62*, S22–S23.
689 https://doi.org/10.1002/pol.1962.1206217338

690 Gnanasambandam, R., & Proctor, A. (2000). Determination of pectin degree of esterification
691 by diffuse reflectance Fourier transform infrared spectroscopy. *Food Chemistry*, *68*(3),
692 327–332. https://doi.org/10.1016/S0308-8146(99)00191-0

693 Grein, A., da Silva, B. C., Wendel, C. F., Tischer, C. A., Sierakowski, M. R., Moura, A. B.
694 D., Iacomini, M., Gorin, P. A. J., Simas-Tosin, F. F., & Riegel-Vidotti, I. C. (2013).

695 Structural characterization and emulsifying properties of polysaccharides of Acacia
696 mearnsii de Wild gum. *Carbohydrate Polymers*, *92*(1), 312–320.
697 https://doi.org/10.1016/j.carbpol.2012.09.041

698 Grein-Iankovski, A., Ferreira, J. G. L., Orth, E. S., Sierakowski, M.-R., Cardoso, M. B.,
699 Simas, F. F., & Riegel-Vidotti, I. C. (2018). A comprehensive study of the relation
700 between structural and physical chemical properties of acacia gums. *Food*
701 *Hydrocolloids*, *85*, 167–175. https://doi.org/10.1016/j.foodhyd.2018.07.011

702 Hallén, A. (1972). Chromatography of acidic glycosaminoglycans on DEAE-cellulose.
703 *Journal of Chromatography A*, *71*(1), 83–91. https://doi.org/10.1016/S0021-
704 9673(01)85691-0

705 Idris, O. H. M., Williams, P. A., & Phillips, G. O. (1998). Characterization of gum from
706 Acacia senegal trees of different age and location using multidetection gel permeation
707 chromatography. *Food Hydrocolloids*, *12*(4), 379–388. https://doi.org/10.1016/S0268-
708 005X(98)00058-7

709 Kačuráková, M., Capek, P., Sasinková, V., Wellner, N., & Ebringerová, A. (2000). FT-IR
710 study of plant cell wall model compounds: pectic polysaccharides and hemicelluloses.
711 *Carbohydrate Polymers*, *43*(2), 195–203. https://doi.org/10.1016/S0144-
712 8617(00)00151-X

713 Karaki, N., Aljawish, A., Muniglia, L., Bouguet-Bonnet, S., Leclerc, S., Paris, C., Jasniewski,
714 J., Humeau-Virot, C. (2017). Functionalization of pectin with laccase-mediated
715 oxidation products of ferulic acid. *Enzyme and Microbial Technology*, *104*, 1–8.
716 https://doi.org/10.1016/j.enzmictec.2017.05.001

717 Karaki, N., Aljawish, A., Muniglia, L., Humeau, C., & Jasniewski, J. (2016). Physicochemical
718 characterization of pectin grafted with exogenous phenols. *Food Hydrocolloids*, *60*,
719 486–493. https://doi.org/10.1016/j.foodhyd.2016.04.004

720 Lewis, B. A., & Smith, F. (1957). The heterogeneity of polysaccharides as revealed by
721 electrophoresis on glass-fiber paper. *Journal of the American Chemical Society*,
722 *79*(14).

723 Mahendran, T., Williams, P. A., Phillips, G. O., Al-Assaf, S., & Baldwin, T. C. (2008). New
724 Insights into the Structural Characteristics of the Arabinogalactan−Protein (AGP)
725 Fraction of Gum Arabic. *Journal of Agricultural and Food Chemistry*, *56*(19), 9269–
726 9276. https://doi.org/10.1021/jf800849a

727 McNamee, B. F., O'Riorda, E. D., & O'Sullivan, M. (1998). Emulsification and
728 Microencapsulation Properties of Gum Arabic. *Journal of Agricultural and Food*
729 *Chemistry*, *46*(11), 4551–4555. https://doi.org/10.1021/jf9803740

730 Nie, S.-P., Wang, C., Cui, S. W., Wang, Q., Xie, M.-Y., & Phillips, G. O. (2013). The core
731 carbohydrate structure of Acacia seyal var. seyal (Gum arabic). *Food Hydrocolloids*,
732 *32*(2), 221–227. https://doi.org/10.1016/j.foodhyd.2012.12.027

733 Nussinovitch, A. (1997). Exudate gums. In A. Nussinovitch (Ed.), *Hydrocolloid Applications:*
734 *Gum technology in the food and other industries* (pp. 125–139). Boston, MA: Springer
735 US.

736 Oostwal, M. G., Blees, M. H., de Bleijser, J., & Leyte, J. C. (1993). Chain self-diffusion in
737 aqueous salt-free solutions of sodium poly(styrenesulfonate). *Macromolecules*, *26*,
738 7300–7308. https://doi.org/10.1021/ma00078a028

739 Padayachee, A., Netzel, G., Netzel, M., Day, L., Zabaras, D., Mikkelsen, D., & Gidley, M. J.
740 (2012). Binding of polyphenols to plant cell wall analogues – Part 1: Anthocyanins.
741 *Food Chemistry*, *134*(1), 155–161. https://doi.org/10.1016/j.foodchem.2012.02.082

742 Picton, L., Bataille, I., Muller, G. (2000). Analysis of a complex polysaccharide (gum arabic)
743 by multi-angle laser light scattering coupled on-line to size exclusion chromatography
744 and flow field flow fractionation. *Carbohydrate Polymers, 42,* 23–31.
745 https://doi.org/10.1016/S0144-8617(99)00139-3

746 Pirestani, S., Nasirpour, A., Keramat, J., Desobry, S., & Jasniewski, J. (2017). Effect of
747 glycosylation with gum Arabic by Maillard reaction in a liquid system on the
748 emulsifying properties of canola protein isolate. *Carbohydrate Polymers*, *157*, 1620–
749 1627. https://doi.org/10.1016/j.carbpol.2016.11.044

750 Ralph, J., Quideau, S., Grabber, J. H., & Hatfield, R. D. (1994). Identification and synthesis of
751 new ferulic acid dehydrodimers present in grass cell walls. *Journal of the Chemical*
752 *Society, Perkin Transactions 1*, (23), 3485–3498.
753 https://doi.org/10.1039/P19940003485

754 Randall, R. C., Phillips, G. O., & Williams, P. A. (1988). The role of the proteinaceous
755 component on the emulsifying properties of gum arabic. *Food Hydrocolloids*, *2*(2),
756 131–140. https://doi.org/10.1016/S0268-005X(88)80011-0

757 Randall, R. C., Phillips, G. O., & Williams, P. A. (1989). Fractionation and characterization
758 of gum from Acacia senegal. *Food Hydrocolloids*, *3*(1), 65–75.
759 https://doi.org/10.1016/S0268-005X(89)80034-7

760 Sajjadi, S. E., Shokoohinia, Y., & Moayedi, N.-S. (2012). Isolation and identification of
761 ferulic acid from aerial parts of *Kelussia odoratissima* Mozaff. *Jundishapur Journal of*
762 *Natural Pharmaceutical Products*, *7*(4), 159–162. https://doi.org/10.17795/jjnpp-4861

763 Sanchez, C., Nigen, M., Mejia Tamayo, V., Doco, T., Williams, P., Amine, C., & Renard, D.
764 (2017). Acacia gum: History of the future. *Food Hydrocolloids*.
765 https://doi.org/10.1016/j.foodhyd.2017.04.008

766 Sanchez, C., Schmitt, C., Kolodziejczyk, E., Lapp, A., Gaillard, C., & Renard, D. (2008). The
767 Acacia Gum Arabinogalactan Fraction Is a Thin Oblate Ellipsoid: A New Model
768 Based on Small-Angle Neutron Scattering and Ab Initio Calculation. *Biophysical*
769 *Journal*, *94*(2), 629–639. https://doi.org/10.1529/biophysj.107.109124

770 Shi, Y., Li, C., Zhang, L., Huang, T., Ma, D., Tu, Z., Wang, H., Xie, H., Zhang, N., Ouyang,
771 B. (2017). Characterization and emulsifying properties of octenyl succinate anhydride
772 modified Acacia seyal gum (gum arabic). *Food Hydrocolloids*, *65*, 10–16.
773 https://doi.org/10.1016/j.foodhyd.2016.10.043

774 Sun, W.-Q., Payne, G. F., Moas, M. S. G. L., Chu, J. H., & Wallace, K. K. (1992). Tyrosinase
775 Reaction/Chitosan Adsorption for Removing Phenols from Wastewater.
776 *Biotechnology Progress*, *8*(3), 179–186. https://doi.org/10.1021/bp00015a002

777 Vuillemin, M. E., Michaux, F., Adam, A. A., Linder, M., Muniglia, L., & Jasniewski, J.
778 (2020). Physicochemical characterizations of gum Arabic modified with oxidation
779 products of ferulic acid. *Food Hydrocolloids*, *107*, 105919.
780 https://doi.org/10.1016/j.foodhyd.2020.105919

781 Wada, S., Ichikawa, H., & Tatsumi, K. (1993). Removal of phenols from wastewater by
782 soluble and immobilized tyrosinase. *Biotechnology and Bioengineering*, *42*(7), 854–
783 858. https://doi.org/10.1002/bit.260420710

784 Wang, H., Williams, P. A., & Senan, C. (2014). Synthesis, characterization and emulsification
785 properties of dodecenyl succinic anhydride derivatives of gum Arabic. *Food*
786 *Hydrocolloids*, *37*, 143–148. https://doi.org/10.1016/j.foodhyd.2013.10.033

787 Williams, P. A., Phillips, G. O., & Stephen, A. M. (1990). Spectroscopic and molecular
788 comparisons of three fractions from Acacia senegal gum. *Food Hydrocolloids*, *4*(4),
789 305–311. https://doi.org/10.1016/S0268-005X(09)80207-5

790 Witayakran, S., & Ragauskas, A. J. (2009). Synthetic Applications of Laccase in Green
791 Chemistry. *Advanced Synthesis & Catalysis*, *351*(9), 1187–1209.
792 https://doi.org/10.1002/adsc.200800775